

# Can Decentralized Control Outperform Centralized? The Role of Communication Latency

Luca Ballotta<sup>ID</sup>, Mihailo R. Jovanović<sup>ID</sup>, *Fellow, IEEE*, and Luca Schenato<sup>ID</sup>, *Fellow, IEEE*

**Abstract**— In this paper, we examine the influence of communication latency on performance of networked control systems. Even though decentralized control architectures offer advantages in terms of communication, maintenance costs, and scalability, it is an open question how communication latency that varies with network topology influences closed-loop performance. For networks in which delays increase with the number of links, we establish the existence of a fundamental performance trade-off that arises from control architecture. In particular, we utilize consensus dynamics with single- and double-integrator agents to show that, if delays increase fast enough, a sparse controller with nearest neighbor interactions can outperform the centralized one with all-to-all communication topology.

**Index Terms**—Communication latency, control architecture, decentralized control, network optimization.

## I. INTRODUCTION

IT IS widely accepted that modern multi-agent systems cannot rely on centralized control architectures. This conclusion stems from issues connected to gathering all decision making to a central node, ranging from lack of robustness and failures proneness, to maintenance costs, to communication overhead. Indeed, large-scale networks have experienced a net shift towards decentralized and distributed architectures in the literature over the past years [22], [36]. Moreover, the recent deployment of powerful communication protocols for massive networks, *e.g.*, 5G [7], [26], and advances in embedded electronics [38], [44], as well as in algorithmic for low-power devices (*e.g.*, TinyML [49]), which allow for spreading complex computational tasks across network nodes according to edge- and fog-computing paradigms [41], [42], [52], are making such networked systems grow at unprecedented sizes and scales, further stressing the importance of distributed controller architectures.

A challenging issue in large-scale networked systems is the latency arising from channel constraints, as limited bandwidth or packet retransmissions. To address such problems, research efforts have been moving towards two main directions.

This work has been partially supported by the CARIPARO Foundation Visiting Programme “HiPER”, by the Italian Ministry of Education, University and Research (MIUR) through the PRIN project no. 2017NS9FEY entitled “Realtime Control of 5G Wireless Networks”, and through the initiative “Departments of Excellence” (Law 232/2016), and by the US National Science Foundation (NSF) under Awards ECCS-1708906 and ECCS-1809833. The views and opinions expressed in this work are those of the authors and do not necessarily reflect those of the funding institutions.

L. Ballotta and L. Schenato are with the Department of Information Engineering, University of Padova, 35131 Padova, Italy {ballotta, schenato}@dei.unipd.it

M. R. Jovanović is with the Ming Hsieh Department of Electrical and Computer Engineering, University of Southern California, Los Angeles, CA 90089 USA mihailo@usc.edu

**Related work in control theory** deals with control design for distributed architectures, where classical methods, such as LQG or  $\mathcal{H}_2/\mathcal{H}_\infty$  control, fail through their intrinsic nature which requires an all-to-all, infeasible communication burden.

A body of works focuses on stability, *e.g.*, [39], [45] are concerned with finite-time delay-dependent stability of discrete-time systems, [6] finds sufficient conditions for uniform stability of linear delay systems, and [9], [13] analyze consensus and error compensation for vehicular platoons. Another line of work deals with maximizing performance for structured controllers, *e.g.*, [18], [33] study  $\mathcal{H}_2$ -norm minimization for time-delay systems, [43] proposes a cyber-physical architecture with LQR for wide-area power systems, [35] develops a procedure for time-varying dead-time compensation by adapting the Filtered Smith Predictor, and [4] investigates sensor-and-processing selection for optimal estimation in star networks.

A more recent trend is designing the controller architecture. For large-scale systems, this leads naturally to sparse network structures, which can tame issues as communication overhead and scalability. This is achieved by introducing penalty terms in the cost function to trade performance for controller complexity, *e.g.*, [2], [27], [28], [30], [31]. In particular, reference [32] proposed the *Regularization for Design* framework, addressing optimization of communication links.

**Related work in optimization theory** is concerned with minimization of distributed cost functions, which are only partially accessible at each agent and possibly reveal themselves overtime. A huge body of works has been devoted to study suitable algorithms, a short list of which is represented by [10], [15], [40], [46], [51]. In particular, a line of work has been concerned specifically with the design of algorithms in the presence of communication delays, the main issues being related to convergence conditions. For example, [17], [21], [47], [53], [54] study consensus of multi-agent systems with additive or multiplicative time-delays under various network topologies and agent dynamics. This approach usually assumes the communication network be given, and focuses on the information exchange and processing by the agents from an optimization standpoint.

**Addressed Problem.** Even though both control design for delay-dependent dynamics and design of controller architectures are well-studied topics, it remains unclear how *network connectivity affects the closed-loop performance in the presence of architecture-dependent communication latency*. When the total available bandwidth does not increase with the size of the network [17] or when multi-hop communication is used for low-power devices [20], the number of active communication links may cause a non-negligible variation of such a latency.

In this case, it is important to take into account increase in delays with the number of links when designing the controller.

Such an approach is conceptually different from the approaches used in literature. On one hand, delay-aware control design and optimization assume structured controllers and do not address architecture-dependent delay variations. On the other hand, architecture designs as in [31], [32] do not quantify the impact of delays on performance and force sparsity by regularizing the optimization problem. In fact, while the fully connected architecture is avoided by designers because of practical limitations, centralized control is usually regarded as an upper bound for performance. We fill this gap by addressing architecture-dependent delays in the dynamics of the controlled system, and analyzing how the optimal performance is affected by variations in such delays.

**Preview of Key Results.** We utilize ring topology with single- and double-integrator agent dynamics to examine fundamental performance limitations in networks with architecture-dependent delays. By exploiting circulant structure of the underlying matrices we demonstrate that the choice of controller architecture has profound impact on network performance in the presence of delays. Among other applications, circulant networks are encountered in source seeking by smart mobile sensors [8], [34] and in target tracking by robots [1], [29].

For a ring topology with  $n$  nearest neighbor interactions, we establish convexity of a minimum-variance control design problem, with respect to the feedback gains, and examine how network connectivity influences the closed-loop performance. When the delays increase fast enough with the number of links, we show that sparse topologies outperform highly connected ones. This is done by exploiting spatially-invariant structure to explicitly quantify impact of network-dependent latency on performance of stochastically-forced networks.

We show that the steady-state variance of a stochastically-forced network,  $J_{\text{tot}}(n)$ , can be represented by a sum of two monotone functions of the number of neighbors  $n$ ,

$$J_{\text{tot}}(n) = J_{\text{network}}(n) + J_{\text{latency}}(n) \quad (\text{I.1})$$

Here,  $J_{\text{network}}(n)$  quantifies impact of control architecture and  $J_{\text{latency}}(n)$  determines influence of communication latency on network performance. While  $J_{\text{network}}(n)$  decreases with  $n$  and is minimized by a fully-connected centralized architecture,  $J_{\text{latency}}(n)$  increases with  $n$ . This demonstrates the presence of a fundamental trade-off: on one hand, feedback control takes advantage of dense topologies that enhance information sharing but, on the other, many communication links induce long delays which has negative impact on network performance. While (I.1) can be derived analytically for ring topology with continuous-time, single-integrator dynamics, our computational experiments show that a similar *centralized-decentralized trade-off* can be observed for general undirected topologies and that, in some cases, the decentralized architecture (by this meaning nearest-neighbor interactions) provides optimal performance.

**Paper Outline.** In Section II we provide models for communication latency and control architecture, and state the minimum-variance control design. In Section III we solve the problem for continuous-time agent dynamics, leveraging the

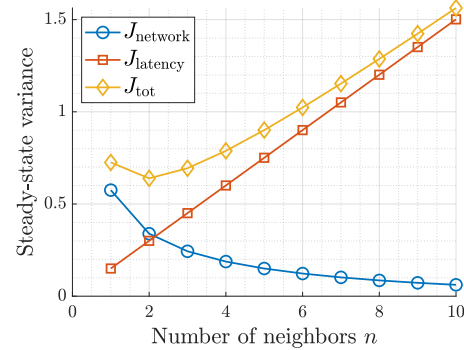


Fig. 1. Steady-state variance  $J_{\text{tot}}(n)$  versus number of neighbors. The variance is the sum of two costs:  $J_{\text{network}}(n)$  represents impact of control architecture, while  $J_{\text{latency}}(n)$  is due to the delays affecting the dynamics.

TABLE I  
OUTLINE OF THEORETICAL TOOLS (ITALIC FONT) AND TECHNICAL RESULTS (ROMAN FONT).

	<b>Model</b>	<b>Stability</b>	<b>Variance</b>
<b>Cont. time (CT)</b>	Single int. (III.1),(II.3)	<i>Scalar SDDEs</i> [24] Closed form (III.4)	<i>Scalar SDDEs</i> [24] Closed form (III.5)
	Double int. (III.7)–(II.4)	<i>Exponential polynomials</i> [5] <i>SDDEs</i> [11], [48] <i>Implicit</i> (III.10)	<i>SDDEs</i> [48], <i>time-scale separation</i> [25] Integral form (III.13) Approximated (III.14)
<b>Disc. time (DT)</b>	Single int. (IV.1),(II.3)	<i>Root locus</i> [50] Closed form (IV.3)	<i>Moment matching w/ Yule-Walker eqs.</i> [14] Recursive (E.2),(E.7)
	Double int. (IV.2)	<i>Jury criterion</i> [23] Closed form (D.4)	<i>Moment matching w/ Yule-Walker eqs.</i> [14] Closed form (E.18)

theory of Stochastic Delay Differential Equations (SDDEs). While analytical results can be obtained for single-integrator dynamics (Section III-A), we also deal with more realistic models such as double integrators in Section III-B. We prove in Section III-C that the proposed design is a convex problem and evaluate it numerically in Section III-D, showing that the performance is optimized by decentralized architectures. In order to address realistic models for communication, we also study discrete-time systems in Section IV and show that the fundamental behavior of the system does not change. Table I summarizes the technical results and the theoretical tools exploited thereto. Final remarks are drawn in Section V.

## II. PROBLEM SETUP

We consider a circular formation with  $N$  agents in which the state of the  $i$ th agent at time  $t$  is given by  $\bar{x}_i(t) \in \mathbb{R}$  with the control input  $u_i(t) \in \mathbb{R}$ . For notational convenience, we introduce the aggregate state of the system  $\bar{x}(t)$  and the aggregate control input  $u(t)$  by stacking states and control inputs of each subsystem  $\bar{x}_i(t)$  and  $u_i(t)$ , respectively.

**Problem Statement.** The agents aim to reach consensus towards a common state trajectory. The  $i$ th component of the vector  $x(t) \doteq \Omega \bar{x}(t)$  represents the mismatch between the state of agent  $i$  and the average network state at time  $t$ , where

$$\Omega \doteq I_N - \frac{\mathbb{1}_N \mathbb{1}_N^\top}{N} \quad (\text{II.1})$$

and  $\mathbb{1}_N \in \mathbb{R}^N$  is the vector of all ones, such that  $\Omega \mathbb{1}_N = 0$ .

**Communication Model.** Data are exchanged in a symmetric fashion through a shared wireless channel so that each agent communicates with its  $2n$  closest neighbors in ring topology.

**Assumption 1** (Communication latency). Agent  $i$  receives state measurements from the  $n < N/2$  agent pairs located  $\ell$  positions ahead and behind in the formation,  $\ell = 1, \dots, n$ . All measurements are received with delay  $\tau_n \doteq f(n)$  where  $f(\cdot)$  is a positive increasing sequence.

**Feedback Control.** Agent  $i$  uses the received information to compute the state mismatches  $y_{i,\ell\pm}(t)$  relative to its neighbors,

$$y_{i,\ell\pm}(t) = \begin{cases} \bar{x}_i(t) - \bar{x}_{i\pm\ell}(t), & 0 < i \pm \ell \leq N \\ \bar{x}_i(t) - \bar{x}_{i\pm\ell+N}(t), & \text{otherwise} \end{cases} \quad (\text{II.2})$$

and the proportional control input is given by

$$u_{P,i}(t) = -\sum_{\ell=1}^n k_{\ell} [(y_{i,\ell+}(t - \tau_n) + y_{i,\ell-}(t - \tau_n))] \quad (\text{II.3})$$

where the measurements are delayed according to Assumption 1.

For networks with double integrator agents, the control input  $u_i(t)$  may also include a derivative term,

$$u_i(t) = \eta u_{P,i}(t) - \eta \frac{d\bar{x}_i(t)}{dt} = \eta u_{P,i}(t) - \eta \frac{dx_i(t)}{dt} \quad (\text{II.4})$$

The derivative term in (II.4) is delay free because it only requires measurements coming from the agent itself, which we assume to be available instantaneously. The proportional input can be compactly written as  $u_P(t) = -K\bar{x}(t - \tau_n) = -Kx(t - \tau_n)$ , with the feedback gain matrix,

$$K = \text{circ} \left( \sum_{\ell=1}^n k_{\ell}, -k_1, \dots, -k_n, 0, \dots, 0, -k_n, \dots, -k_1 \right) \quad (\text{II.5})$$

where  $\text{circ}(a_1, \dots, a_n)$  denotes the circulant matrix in  $\mathbb{R}^{n \times n}$  with elements  $a_1, \dots, a_n$  in the first row.

**Problem 1.** Design the feedback gains in order to minimize the steady-state variance of the consensus error,

$$\text{P control: } \underset{K}{\operatorname{argmin}} \sigma^2(K) \quad (\text{II.6a})$$

$$\text{PD control: } \underset{\eta, K}{\operatorname{argmin}} \sigma^2(\eta, K) \quad (\text{II.6b})$$

where

$$\sigma^2 \doteq \lim_{t \rightarrow +\infty} \mathbb{E} [\|x(t)\|^2] \quad (\text{II.7})$$

and  $\mathbb{E}[x(\cdot)] \equiv \mathbb{E}[x(0)] = 0$  is assumed w.l.o.g..

### III. CONTINUOUS-TIME AGENT DYNAMICS

We first examine continuous-time models with single- (Section III-A) and double-integrator (Section III-B) agent dynamics. In Section III-C we address the minimum-variance control design problem, in Section III-D we conduct computational experiments, and in Section III-E we explicitly quantify the impact of delay on the performance of distributed and centralized control strategies.

#### A. Single Integrator Model

The dynamics of the  $i$ th agent are described by the first-order differential equation driven by standard Brownian noise  $\bar{w}_i(\cdot)$ :

$$d\bar{x}_i(t) = u_{P,i}(t)dt + d\bar{w}_i(t) \quad (\text{III.1})$$

and the network error dynamics are

$$dx(t) = -Kx(t - \tau_n)dt + dw(t) \quad (\text{III.2})$$

where the process noise is given by  $dw(t) \sim \mathcal{N}(0, \Omega\Omega^T dt)$ . Exploiting symmetry of the matrix  $K$ , we employ the change of variables  $x(t) = T\tilde{x}(t)$ , with  $K = T\Lambda T^T$ , to obtain  $N$  decoupled scalar subsystems with state  $\tilde{x}_j(t)$ ,  $j = 1, \dots, N$ ,

$$d\tilde{x}_j(t) = -\lambda_j \tilde{x}_j(t - \tau_n)dt + d\tilde{w}_j(t) \quad (\text{III.3})$$

where  $\lambda_j$  is the  $j$ th eigenvalue of  $K$ . The subsystem with  $\lambda_1 = 0$  has trivial dynamics, *i.e.*,  $d\tilde{x}_1(t) \equiv 0$ , with initial condition  $\tilde{x}_1(0) = 0$  by construction. For  $j \neq 1$ , subsystem (III.3) is a single integrator driven by standard Brownian noise.

**Stability Analysis.** Mean-square stability of scalar stochastic differential equations of the form (III.3) has been addressed in the literature. We build on the classical result in [24] to characterize consensus stability for the multi-agent formation.

**Proposition 1** (Stability of CT single integrators). *The network error  $x(t)$  is mean-square stable if and only if*

$$\lambda_j \in \left( 0, \frac{\pi}{2\tau_n} \right), \quad j = 2, \dots, N. \quad (\text{III.4})$$

*In this case,  $x(t)$  is a Gaussian process and its steady-state variance is determined by*

$$\sigma^2(K) = \sum_{j=2}^N \sigma_I^2(\lambda_j), \quad \sigma_I^2(\lambda_j) = \frac{1 + \sin(\lambda_j \tau_n)}{2\lambda_j \cos(\lambda_j \tau_n)} \quad (\text{III.5})$$

*where we make explicit the dependence of  $\sigma^2$  on  $K$  and  $\sigma_I^2(\lambda_j)$  is the variance of the trivial solution of (III.3).*

*Sketch of Proof.* In view of the decoupling, stability of (III.2) amounts to stability of all subsystems (III.3),  $j = 1, \dots, N$ , with the variances of  $x(t)$  and  $\tilde{x}(t)$  being equal. Condition (III.4) and expression (III.5) have been derived in [24].  $\square$

While the variance of delay-free systems is bounded for any positive eigenvalues  $\lambda_2, \dots, \lambda_N$ , the presence of delay constrains a stabilizing control according to (III.4). In fact, longer delays  $\tau_n$  induce smaller upper bounds on the eigenvalues.

The following result will turn useful in the control design.

**Corollary 1.** *Let  $\lambda$  satisfy (III.4). Then the function  $\sigma_I^2(\lambda)$  is strictly convex and its point of minimum  $\lambda^*$  is given by*

$$\lambda^* = \frac{\beta^*}{\tau_n}, \quad \beta^* = \cos \beta^* \quad (\text{III.6})$$

*Proof.* Follows from standard computations over the derivatives of  $\sigma_I^2(\cdot)$ . See Appendices A-B in the preprint [3].  $\square$

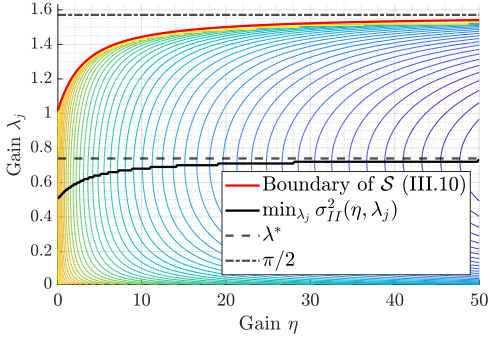


Fig. 2. Level curves of the steady-state variance for the continuous-time double integrator (III.9) and points of minimum with fixed derivative gain.

### B. Double Integrator Model

We now examine networks in which each agent obeys a second-order dynamics with the PD control input (II.4):

$$\frac{d^2\bar{x}_i(t)}{dt^2} = u_i(t) + \frac{d\bar{w}_i(t)}{dt} \quad (\text{III.7})$$

For simplicity, we normalize the delay by scaling (III.7) as

$$\bar{x}_i(\cdot) \leftarrow \bar{x}_i(\tau_n \cdot), \quad \eta \leftarrow \tau_n \eta, \quad k_\ell \leftarrow \tau_n k_\ell, \quad \bar{w}_i(\cdot) \leftarrow \tau_n \bar{w}_i(\cdot) \quad (\text{III.8})$$

Stacking the agent errors and their derivatives in the formation vector, the error dynamics can be decoupled as before, yielding

$$\frac{d^2\tilde{x}_j(t)}{dt^2} = -\eta \frac{d\tilde{x}_j(t)}{dt} - \eta \lambda_j \tilde{x}_j(t-1) + \frac{d\tilde{w}_j(t)}{dt} \quad (\text{III.9})$$

**Stability Analysis.** We have the following result.

**Proposition 2** (Stability of CT double integrators). *The network error  $x(t)$  is mean-square stable if*

$$\lambda_j \in \left(0, \frac{\beta}{\sin \beta}\right), \quad \eta = \beta \tan \beta, \quad \beta \in \left(0, \frac{\pi}{2}\right), \quad j = 2, \dots, N. \quad (\text{III.10})$$

Condition (III.10) can be equivalently written as

$$(\eta, \lambda_j) \in \mathcal{S} \doteq \{(\eta, \lambda_j) \in \mathbb{R}_+^2 : \lambda_j < \phi(\eta)\}, \quad j = 2, \dots, N \quad (\text{III.11})$$

where the implicit function  $\phi(\cdot)$  is concave increasing and

$$\phi(0) = 1, \quad \lim_{\eta \rightarrow +\infty} \phi(\eta) = \frac{\pi}{2} \quad (\text{III.12})$$

If  $\exists j \neq 1 : (\eta, \lambda_j) \notin \overline{\mathcal{S}}$ , the system is mean-square unstable.

*Proof.* See Appendix A.  $\square$

Similar to the single-integrator case, Proposition 2 states that the presence of delay requires more restrictive conditions than positive gains. In words, the system is stable if the instantaneous component of the control input in (II.4) is sufficiently “strong” compared to the delayed one. The steady-state variance of  $\tilde{x}_j(t)$  for  $j \neq 1$  can be computed using [48, Section 4],

$$\sigma_{II}^2(\eta, \lambda_j) = \frac{1}{2\pi} \int_{-\infty}^{+\infty} \frac{d\omega}{|-\omega^2 + j\eta\omega + \eta\lambda_j e^{-j\omega}|^2} \quad (\text{III.13})$$

and  $\sigma^2 = \sigma^2(\eta, K) = \sum_{j=2}^N \sigma_{II}^2(\eta, \lambda_j)$ . A graphical illustration of the level curves of  $\sigma_{II}^2(\eta, \lambda_j)$  is provided in Fig. 2.

**Model Approximation.** As shown in Appendix B, when the feedback gain  $\eta$  is sufficiently high, separation of time scales allows us to approximate (III.9) with the first-order dynamics,

$$d\tilde{x}_j(t) = -\lambda_j \tilde{x}_j(t-1) dt + dn(t) \quad (\text{III.14})$$

where the variance of Brownian motion  $n(t)$  is inversely proportional to  $\eta$ . In words, when the damping is high enough, the derivative of  $\tilde{x}_j(t)$  converges to zero much quicker than  $\tilde{x}_j(t)$ , which represents the dominant component of the dynamics. Utility of this approximation is illustrated in Fig. 2: with fixed  $\bar{\eta}$ , the point of minimum of the corresponding 1D variance curve, *i.e.*,  $\operatorname{argmin}_{\lambda_j} \sigma_{II}^2(\bar{\eta}, \lambda_j)$  (solid black line), approaches the minimizer  $\lambda^*$  of the single integrator model (dashed black, see Corollary 1) as  $\bar{\eta}$  grows. We also note that the variance decreases with  $\eta$ .

### C. Control Design

**Single Integrator Model.** For system (III.2) Problem 1 amounts to

$$k_1^*, \dots, k_n^* = \operatorname{argmin}_{\{k_\ell\}_{\ell=1}^n} \sigma^2(K) \quad (\text{III.15})$$

and parameterization (III.3) allows to rewrite it as

$$k_1^*, \dots, k_n^* = \operatorname{argmin}_{\{k_\ell\}_{\ell=1}^n} \sum_{j=2}^N \sigma_I^2(\lambda_j) \quad (\text{III.16})$$

where the circulant matrix  $K$  is uniquely defined by its eigenvalues [19] and the stability condition is given by (III.4). Linear dependence of the eigenvalues of  $K$  on the feedback gains [19] and Corollary 1 guarantee convexity of optimization problem (III.16). Thus, the optimal feedback gains can be computed efficiently. To make analytical progress and gain intuition, we also consider the following approximation of (III.16),

$$\tilde{k}_1^*, \dots, \tilde{k}_n^* = \operatorname{argmin}_{\{k_\ell\}_{\ell=1}^n} \sum_{j=2}^N (\lambda_j - \lambda^*)^2 \quad (\text{III.17})$$

which forces the spectrum of  $K$  to squeeze about the “optimal” eigenvalue  $\lambda^*$ . The variance  $\sigma_I^2(\cdot)$  can be approximated with a quadratic function around its minimum because it is strictly convex, differentiable in the stability region, and it blows up at the boundaries  $\{0, \pi/2\}$ , see Fig. 3.

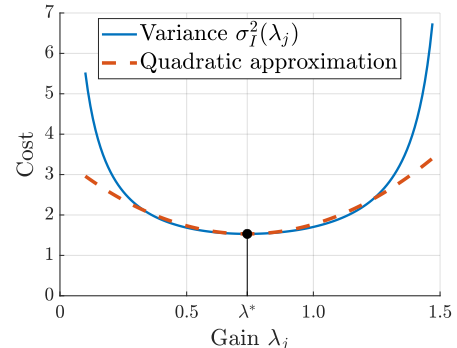


Fig. 3. Exact variance function (III.5) and its quadratic approximation.

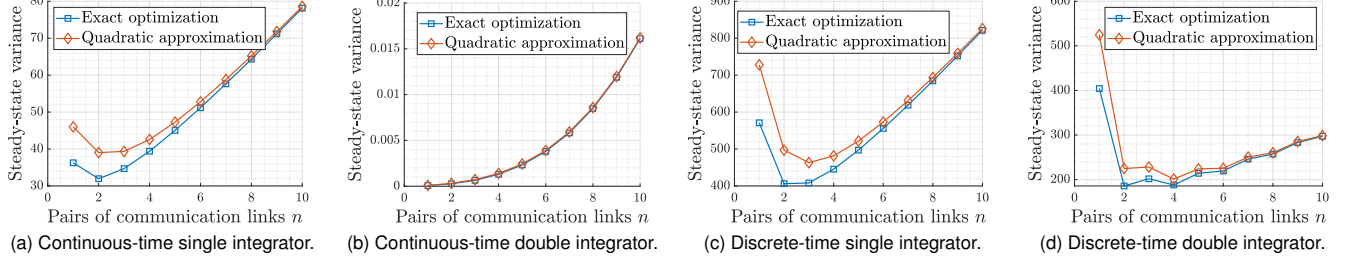


Fig. 4. Optimal and suboptimal steady-state scalar variances with linear delay increase for different agent dynamics.

**Proposition 3** (Near-optimal proportional control). *The solution of problem (III.17) is determined by*

$$\tilde{k}_\ell^* \equiv \tilde{k}^* \doteq \frac{\lambda^*}{2n+1}.$$

*Proof.* The result follows by applying properties of the DFT to (III.17); see Appendices C-D in [3] for details.  $\square$

Proposition 3 shows that spatially-constant feedback gains provide good performance even when spatially-varying feedback gains are allowed. According to Corollary 1, the suboptimal gain  $\tilde{k}^*$  decreases with the delay  $\tau_n$  and with the number of agents involved in the feedback loops, thereby reflecting benefits of communication.

**Double Integrator Model.** Approximation (III.14) and Fig. 2 show that, for sufficiently large  $\eta$ , the variance of the double-integrator subsystem (III.9) has structure similar to the single integrator, *i.e.*,  $\sigma_H^2(\eta, \lambda_j) \approx c\sigma_I^2(\lambda_j)$  for some “small”  $c > 0$ . Thus, we approximate the control design (II.6b) as

$$\tilde{\eta}^*, \arg\min_{\{k_\ell\}_{\ell=1}^n} \sum_{j=2}^N \sigma_I^2(\lambda_j) \quad (\text{III.18})$$

where  $\tilde{\eta}^*$  is chosen beforehand so that the time-scale separation argument provides a reasonable approximation (III.14). In particular, the optimization problem for proportional feedback gains in (III.18) coincides with the control design for single integrators (III.16), with the exception that the stability condition is now given by  $\lambda_j < \phi(\tilde{\eta}^*)$ ,  $j = 2, \dots, N$ ; see (III.11).

**Remark 1** (Gain scaling). The optimal feedback gains  $\{k_\ell^*\}_{\ell=1}^n$  and  $\tilde{\eta}^*$  are to be scaled by  $1/\tau_n$  according to (III.8).

**Remark 2** (Optimal design for double integrators). Local minimizer of the original optimization problem approximated by (III.18) can be solved using the gradient-based method proposed in [18]. However, this approach does not offer any analytical insight and it does not have any guarantees of computing the globally optimal solution. In contrast, the use of a strictly convex approximation (III.18) allows us to draw a parallel to the optimal design for the single-integrator model and provide insight into a centralized-decentralized trade-off.

#### D. Computational Experiments

Figure 4a shows the minimum variance resulting from the solution of the single-integrator problem (III.15) and the output of the quadratic approximation (III.17) for a network with  $N = 50$  nodes. The centralized-decentralized trade-off is

reflected in the fact that providing additional information to the local feedback loops is advantageous as long as the delay in the dynamics is kept below a certain threshold. Beyond this, poor stabilizability properties induced by long delays constrain the feedback action and diminish benefits of communication. Furthermore, additional computational experiments performed with different rates  $f(\cdot)$  show that the optimal number of links increases for slower rates; for example, the optimal number of links is larger for  $f(n) = \sqrt{n}$  than for  $f(n) = n$ .

For a linear increase in the delay, Fig. 4b shows that the use of approximation (III.18) with  $\tilde{\eta}^* = 70$  identifies nearest-neighbor information exchange as the near-optimal architecture for a double-integrator model. This can be explained by noting that the variance of the process noise  $n(\cdot)$  in the reduced model (III.14) is proportional to  $1/\eta$  and thereby to  $\tau_n$ , according to (III.8), making the variance scale with the delay.

Figures 4c–4d show the result of the same optimization for discrete-time systems. The oscillations about the minimum in Fig. 4d are compatible with the investigated centralized-decentralized trade-off: in general, the sum of two monotone functions does not need to have a unique local minimum. Details about discrete-time systems are provided in Section IV.

**General Symmetric Network Topology.** Even though we primarily focus on ring topology, the control design can be readily extended to general networks with symmetric feedback gain matrices  $K$ . For the single integrator model, this reads

$$K^* = \arg\min_K \sigma^2(K). \quad (\text{III.19})$$

The steady-state network error variance  $\sigma^2(K)$  is a convex function if and only if  $\sigma_I^2(\lambda_j)$  is convex [12], which is proved in Corollary 1 for continuous-time and in Appendix E for discrete-time systems. The optimal gains can then be found numerically via gradient-based methods, where gradients of the eigenvalues can be computed using [37] or [16]. On the other hand, the derivative feedback gain in  $\sigma_H^2(\eta, \lambda_j)$  prevents us from establishing convexity for second-order systems in general. However, if  $\sigma_H^2(\eta, \lambda_j)$  is convex in each coordinate<sup>1</sup>, the design problem can be solved by alternatively optimizing proportional and derivative gains and the centralized-decentralized trade-off can be studied irrespective of the particular topology.

Figure 5 shows the optimization results for a random graph topology obtained using a discrete-time single integrator model with a linear increase in the delay,  $\tau_n = n$ . Here,  $n$  denotes the number of communication hops in the “original”

<sup>1</sup>This can be checked for discrete-time double integrators, see Appendix E.

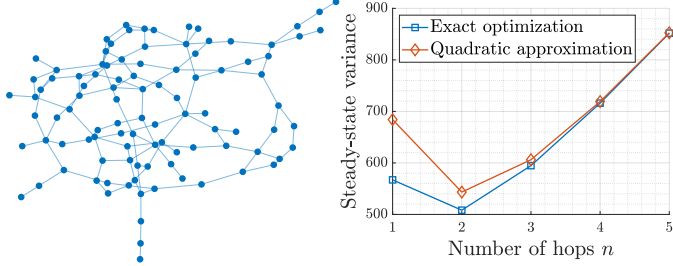


Fig. 5. General network topology (left) and the associated optimal closed-loop variance (right).

network, shown in Fig. 5: as  $n$  increases, each node can first communicate with its nearest neighbors, then with its neighbors' neighbors, and so on. For a control architecture that utilizes different feedback gains for each communication link (*i.e.*, we only require  $K = K^\top$ ) we demonstrate that, in this case, two communication hops provide optimal closed-loop performance.

#### E. Centralized-Distributed Trade-Off: an Analytical Insight

For a single integrator model in continuous time, the centralized-decentralized trade-off can be explicitly quantified by utilizing Proposition 3 to compute the feedback gains and rewriting the objective function as the product

$$\sigma^2 = \underbrace{f(n)}_{\tilde{J}_{\text{latency}}(n)} \cdot \underbrace{\sum_{j=2}^N \tilde{C}_j^*(n)}_{\tilde{J}_{\text{network}}(n)} \quad (\text{III.20})$$

where  $\sigma_I^2(\tilde{\lambda}_j^*) = \tilde{C}_j^*(n)\tau_n$  and  $\tilde{C}_j^*(n)$  only depends on  $n$  and can be computed exactly; see Appendix C. This holds because the suboptimal eigenvalues have expression  $\tilde{\lambda}_j^* = \tilde{c}_j^*(n)\lambda^*$ ; cf. Proposition 3. Such a decomposition can be interpreted as a decoupling of the impact of network ( $\tilde{c}_j^*(n)$ ) and latency ( $\lambda^*$ ) effects on the control design. By inspection, it can be seen that  $\tilde{J}_{\text{network}}(n)$  is a decreasing function of  $n$  and that  $\tilde{J}_{\text{latency}}(n)$  is determined by  $f(n)$ . Furthermore, for sublinear rates  $f(\cdot)$ , the steady-state variance can be also written according to (I.1),

$$\sigma^2 = f(n) \cdot \underbrace{\sum_{j=2}^N (\tilde{C}_j^*(n) - C^*)}_{J_{\text{network}}(n)} + \underbrace{(N-1)C^*f(n)}_{J_{\text{latency}}(n)} \quad (\text{III.21})$$

where  $\sigma_I^2(\lambda^*) = C^*\tau_n$  is the optimal variance according to (III.5) and Corollary 1. Indeed, the summation decreases with superlinear rate, so that  $J_{\text{network}}(n)$  is a decreasing sequence. The terms in  $J_{\text{network}}(n)$ , each associated with a decoupled subsystem (III.3), illustrate benefits of communication: as  $n$  increases, the eigenvalues of  $K$  have more degrees of freedom and can squeeze more tightly about  $\lambda^*$ , reducing performance gaps between subsystems and theoretical optimum. We note that  $J_{\text{network}}(n)$  vanishes for the fully connected architecture.

Even though analytical expressions could not be obtained for minimum-variance designs, the curves in Fig. 4 exhibit trade-offs which are consistent with the above analysis.

#### IV. DISCRETE-TIME SYSTEMS

Finally, we consider discrete-time agent dynamics to illustrate that the afore-established fundamental trade-offs hold in this case as well. In what follows, we denote the discrete time instants as  $\{k\}_{k \in \mathbb{N}} \doteq \{kT_s\}_{k \in \mathbb{N}}$ , where  $T_s$  is the sampling time. Similarly, we re-define the discrete delay as the number of delay steps  $\tau_n \doteq \lceil \tau_n/T_s \rceil$ .

**Agent Models.** The discrete-time versions of the agent dynamics considered in Section III are given by

$$\bar{x}_i(k+1) = \bar{x}_i(k) + u_{P,i}(k) + \bar{w}_i(k) \quad (\text{IV.1})$$

for the single-integrator model, with  $\bar{w}_i(\cdot) \sim \mathcal{N}(0, 1)$ , and

$$\begin{aligned} \bar{x}_i(k+1) &= \bar{x}_i(k) + \bar{z}_i(k) \\ \bar{z}_i(k+1) &= (1 - \eta)\bar{z}_i(k) + \eta u_{P,i}(k) + \bar{w}_i(k) \end{aligned} \quad (\text{IV.2})$$

for the double-integrator model, with  $u_{P,i}(k)$  defined in (II.3).

**Stability Analysis.** The formation error dynamics can be decoupled analogously to the continuous-time models. The decoupled subsystems are asymptotically stable if and only if all the roots of their associated characteristic polynomials lie inside the unit circle in the complex plane.

In general, given a delay  $\tau_n$ , stability conditions with respect to the control gains can be derived in the form of polynomial inequalities through the Jury criterion. For the single-integrator case, one simple condition can be computed analytically.

**Proposition 4** (Stability of DC single integrators). *The network error  $x(t)$  is mean-square stable if and only if*

$$\lambda_j \in \left(0, 2 \sin \left(\frac{\pi}{2} \frac{1}{2\tau_n + 1}\right)\right), \quad j = 2, \dots, N \quad (\text{IV.3})$$

The upper bound in (IV.3) approaches its continuous-time counterpart (III.4) from below as the delay steps tend to infinity (see Fig. 6). A discussion on general stability conditions and the proof of Proposition 4 are provided in Appendix D. The basic argument is the same as for the continuous-time case.

**Performance Evaluation.** With fixed parameters, the steady-state variance of each decoupled subsystem can be computed numerically via the Wiener–Khintchine formula. Also, for any given value of  $\tau_n$ , a closed-form expression can be obtained via moment matching; see Appendix E. Such closed-form expressions have been used for our computational experiments illustrated in Fig. 4. Figure 7 shows the typical variance profiles for the decoupled subsystems.

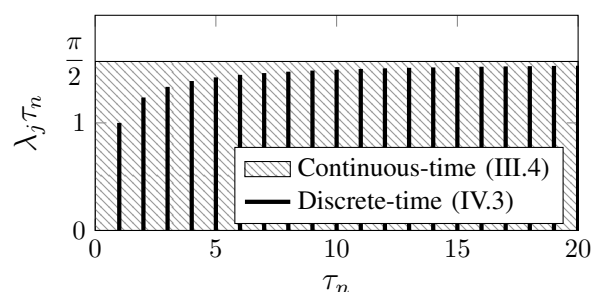


Fig. 6. Stability regions of decoupled single integrators.

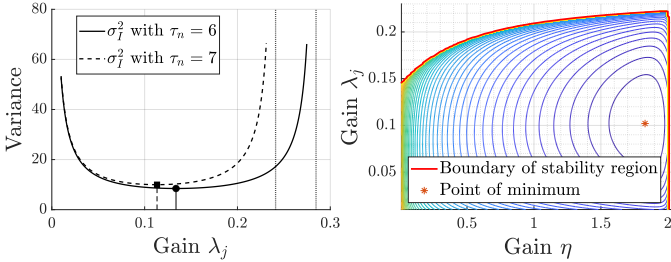


Fig. 7. Typical profiles of the steady-state variance for decoupled discrete-time single integrators (left) and double integrators (right).

## V. CONCLUSION

We study minimum-variance control design for circular formations with both continuous- and discrete-time agent dynamics. We demonstrate that a fundamental trade-off arises when the delay in the dynamics increases with the number of links. In particular, we show that distributed control architectures can offer superior performance to centralized ones that utilize all-to-all information exchange. Several avenues can be considered for future work: for example, the centralized-decentralized trade-off may be further investigated under multiple, stochastic or time-varying delays, unreliable communication, or heterogeneous agents with different delay functions.

## REFERENCES

- [1] L. B. Arranz, A. Seuret, and C. C. De Wit. Translation control of a fleet circular formation of auvs under finite communication range. In *Proc. 48h IEEE Conf. on Decision and Control and 28th Chinese Control Conf.*, pages 8345–8350, 2009.
- [2] M. S. Bahavarnia and N. Motee. Sparse memoryless LQR design for uncertain linear time-delay systems. *Proc. 20th IFAC World Congress*, 50(1):10395–10400, 2017.
- [3] L. Ballotta, M. R. Jovanović, and L. Schenato. Optimal Network Topology of Multi-Agent Systems subject to Computation and Communication Latency (with proofs). *arXiv:2101.10394*, Jan. 2021.
- [4] L. Ballotta, L. Schenato, and L. Carloni. Computation-communication trade-offs and sensor selection in real-time estimation for processing networks. *IEEE Trans. Netw. Sci. Eng.*, 7(4):2952–2965, 2020.
- [5] M. Baptistini and P. Taboas. On the stability of some exponential polynomials. *J. of Mathematical Analysis and Applications*, 205(1):259–272, 1997.
- [6] L. Berezansky, J. Diblík, Z. Svoboda, and Z. Šmarda. Simple uniform exponential stability conditions for a system of linear delay differential equations. *Applied Mathematics and Computation*, 250:605 – 614, 2015.
- [7] A. Biral, M. Centenaro, A. Zanella, L. Vangelista, and M. Zorzi. The challenges of m2m massive access in wireless cellular networks. *Digital Communications and Networks*, 1(1):1–19, 2015.
- [8] L. Brifón-Arranz, L. Schenato, and A. Seuret. Distributed source seeking via a circular formation of agents under communication constraints. *IEEE Control Netw. Syst.*, 3(2):104–115, 2015.
- [9] H. Chehardoli and A. Ghasemi. Formation control of longitudinal vehicular platoons under generic network topology with heterogeneous time delays. *J. of Vibration and Control*, 25(3):655–665, 2019.
- [10] T. Chen, Q. Ling, and G. B. Giannakis. An online convex optimization approach to proactive network resource allocation. *IEEE Trans. Signal Process.*, 65(24):6350–6364, 2017.
- [11] R. Datko. A procedure for determination of the exponential stability of certain differential-difference equations. *Quarterly of Applied Mathematics*, 36(3):279–292, 1978.
- [12] C. Davis. All convex invariant functions of Hermitian matrices. *Archiv der Mathematik*, 8(4):276–278, 1957.
- [13] F. de Oliveira Souza, L. A. B. Torres, L. A. Mozelli, and A. A. Neto. Stability and formation error of homogeneous vehicular platoons with communication time delays. *IEEE Trans. Intell. Transp. Syst.*, 21(10):4338–4349, 2020.
- [14] D. R. Derryberry. *The Yule–Walker Equations and the Partial Autocorrelation Function*, pages 169–179. John Wiley & Sons, Ltd, 2014.
- [15] P. Di Lorenzo and G. Scutari. Distributed nonconvex optimization over time-varying networks. In *Proc. 2016 IEEE Int. Conf. on Acoustics, Speech and Signal Processing*, pages 4124–4128, 2016.
- [16] M. I. Friswell. The derivatives of repeated eigenvalues and their associated eigenvectors. *J. of Vibration and Acoustics*, 118(3):390–397, 07 1996.
- [17] E. Garcia, Y. Cao, and D. W. Casbeer. Periodic event-triggered synchronization of linear multi-agent systems with communication delays. *IEEE Trans. Autom. Control*, 62(1):366–371, 2016.
- [18] M. A. Gomez, A. V. Egorov, S. Mondié, and W. Michiels. Optimization of the  $\mathcal{H}_2$  norm for single-delay systems, with application to control design and model approximation. *IEEE Trans. Autom. Control*, 64(2):804–811, 2019.
- [19] R. M. Gray. Toeplitz and circulant matrices: A review. *Foundations and Trends® in Communications and Information Theory*, 2(3):155–239, 2006.
- [20] G. R. Gupta and N. Shroff. Delay analysis for multi-hop wireless networks. In *IEEE INFOCOM 2009*, pages 2356–2364, 2009.
- [21] C. N. Hadjicostis and T. Charalambous. Average consensus in the presence of delays in directed graph topologies. *IEEE Trans. Autom. Control*, 59(3):763–768, 2014.
- [22] M. R. Jovanović and N. K. Dhingra. Controller architectures: Tradeoffs between performance and structure. *European J. of Control*, 30:76–91, 2016.
- [23] E. I. Jury. A simplified stability criterion for linear discrete systems. *Proc. of the IRE*, 50(6):1493–1500, 1962.
- [24] U. Küchler and B. Mensch. Langevin stochastic differential equation extended by a time-delayed term. *Stochastics and Stochastic Reports*, 40(1-2):23–42, 1992.
- [25] H. K. Khalil. *Nonlinear Systems*. Pearson Education. Prentice Hall, 2002.
- [26] S. Li, L. Da Xu, and S. Zhao. 5G internet of things: A survey. *J. of Industrial Information Integration*, 10:1–9, 2018.
- [27] F. Lian, A. Chakrabortty, and A. Duel-Hallen. Game-theoretic multi-agent control and network cost allocation under communication constraints. *IEEE J. Sel. Areas Commun.*, 35(2):330–340, 2017.
- [28] F. Lin, M. Fardad, and M. R. Jovanović. Design of optimal sparse feedback gains via the alternating direction method of multipliers. *IEEE Trans. Autom. Control*, 58(9):2426–2431, 2013.
- [29] L. Ma and N. Hovakimyan. Cooperative target tracking in balanced circular formation: Multiple uavs tracking a ground vehicle. In *Proc. 2013 American Control Conf.*, pages 5386–5391. IEEE, 2013.
- [30] P. R. Massenio, G. Rizzello, D. Naso, F. L. Lewis, and A. Davoudi. Data-driven optimal structured control for unknown symmetric systems. In *IEEE 16th Int. Conf. on Autom. Sci. Eng.*, pages 179–184, 2020.
- [31] N. Matni. Communication delay co-design in  $\mathcal{H}_2$ -distributed control using atomic norm minimization. *IEEE Control Netw. Syst.*, 4(2):267–278, 2017.
- [32] N. Matni and V. Chandrasekaran. Regularization for design. *IEEE Trans. Autom. Control*, 61(12):3991–4006, 2016.
- [33] W. Michiels, G. Hilhorst, G. Pipeleers, and J. Swevers. *Model Order Reduction for Time-Delay Systems, with Application to Fixed-Order  $\mathcal{H}_2$  Optimal Controller Design*, pages 45–66. Springer International Publishing, Cham, 2016.
- [34] B. J. Moore and C. Canudas-de Wit. Source seeking via collaborative measurements by a circular formation of agents. In *Proc. 2010 American Control Conf.*, pages 6417–6422. IEEE, 2010.
- [35] M. M. Morato and J. E. Normey-Rico. A novel unified method for time-varying dead-time compensation. *ISA Trans.*, 108:78–95, 2021.
- [36] A. Nedić, A. Olshevsky, and M. G. Rabbat. Network topology and communication-computation tradeoffs in decentralized optimization. *Proc. of the IEEE*, 106(5):953–976, 2018.
- [37] R. B. Nelson. Simplified calculation of eigenvector derivatives. *AIAA J.*, 14(9):1201–1205, 1976.
- [38] NVIDIA. Nvidia jetson nano datasheet, 2020. <https://developer.nvidia.com/embedded/jetson-nano>.
- [39] H. Ren, G. Zong, L. Hou, and Y. Yang. Finite-time resilient decentralized control for interconnected impulsive switched systems with neutral delay. *ISA Trans.*, 67:19–29, 2017.
- [40] S. Shahrampour and A. Jadbabaie. Distributed online optimization in dynamic environments using mirror descent. *IEEE Trans. Autom. Control*, 63(3):714–725, 2018.
- [41] W. Shi, J. Cao, Q. Zhang, Y. Li, and L. Xu. Edge computing: Vision and challenges. *IEEE Internet Things J.*, 3(5):637–646, 2016.

[42] W. Shi, S. Zhou, Z. Niu, M. Jiang, and L. Geng. Joint device scheduling and resource allocation for latency constrained wireless federated learning. *IEEE Trans. Wireless Commun.*, 20(1):453–467, 2020.

[43] D. Soudabkhsh, A. Chakraborty, and A. M. Annaswamy. A delay-aware cyber-physical architecture for wide-area control of power systems. *Control Engineering Practice*, 60:171–182, 2017.

[44] A. Suleiman, Z. Zhang, L. Carbone, S. Karaman, and V. Sze. Navion: A 2-mw fully integrated real-time visual-inertial odometry accelerator for autonomous navigation of nano drones. *IEEE J. Solid-State Circuits*, 54(4):1106–1119, 2019.

[45] S. Sun, H. Zhang, W. Li, and Y. Wang. Time-varying delay-dependent finite-time boundedness with  $\mathcal{H}_\infty$  performance for markovian jump neural networks with state and input constraints. *Neurocomputing*, 423:419–426, 2021.

[46] T. Tatarenko and B. Touri. Non-convex distributed optimization. *IEEE Trans. Autom. Control*, 62(8):3744–3757, 2017.

[47] K. I. Tsianos and M. G. Rabbat. Distributed consensus and optimization under communication delays. In *Proc. 49th Allerton Conf. Commun., Control, Comput.*, pages 974–982, 2011.

[48] Z. Wang, X. Li, and J. Lei. Second moment boundedness of linear stochastic delay differential equations. *Discrete and Continuous Dynamical Systems - B*, 19(9):2963 – 2991, 2014.

[49] P. Warden and D. Situnayake. *TinyML: Machine Learning with TensorFlow Lite on Arduino and Ultra-Low-Power Microcontrollers*. O'Reilly Media, 2019.

[50] L. C. Westphal. *Root locus methods for analysis and design*, pages 389–403. Springer US, Boston, MA, 2001.

[51] L. Xiao, S. Boyd, and S.-J. Kim. Distributed average consensus with least-mean-square deviation. *J. of Parallel and Distributed Computing*, 67(1):33–46, 2007.

[52] S. Yi, C. Li, and Q. Li. A survey of fog computing: concepts, applications and issues. In *Proc. ACM Workshop on Mobile Big Data*, pages 37–42, 2015.

[53] X. Zong, T. Li, G. Yin, L. Y. Wang, and J.-F. Zhang. Stochastic controllability of linear systems with time delays and multiplicative noises. *IEEE Trans. Autom. Control*, 63(4):1059–1074, April 2018.

[54] X. Zong, T. Li, and J.-F. Zhang. Consensus conditions of continuous-time multi-agent systems with time-delays and measurement noises. *Automatica*, 99:412–419, 2019.

## APPENDIX

### A. Proof of Proposition 2

The error dynamics equation with agent model (III.7) reads

$$dx(t) = (A_0x(t) + A_1x(t-1))dt + B\bar{w}(t) \quad (A.1)$$

$$A_0 = \begin{bmatrix} 0 & I \\ 0 & -\eta I \end{bmatrix}, \quad A_1 = \begin{bmatrix} 0 & 0 \\ -\eta K & 0 \end{bmatrix}, \quad B = \begin{bmatrix} 0 \\ I \end{bmatrix}$$

with  $\bar{w}(t)$  standard  $N$ -dimensional Brownian motion. The decoupling (III.9) is obtained from (A.1) through the change of basis  $x(t) = (T \otimes I_2)\tilde{x}(t)$ . Rewriting (III.9) as a double integrator in state-space form with state  $\tilde{s}_j(\cdot)$  yields

$$d\tilde{s}_j(t) = (F_0\tilde{s}_j(t) + F_1\tilde{s}_j(t-1))dt + Gd\bar{w}_j(t) \quad (A.2)$$

$$F_0 = \begin{bmatrix} 0 & 1 \\ 0 & -\eta \end{bmatrix}, \quad F_1 = \begin{bmatrix} 0 & 0 \\ -\eta\lambda_j & 0 \end{bmatrix}, \quad G = \begin{bmatrix} 0 \\ 1 \end{bmatrix}$$

Stability of (A.1) is equivalent to that of (A.2) for all  $j$ . In the following, we drop the subscript  $j$  for the sake of readability. For positive eigenvalues  $\lambda$ , (A.2) is mean-square asymptotically stable if  $\alpha_0 < 0$  and unstable if  $\alpha_0 > 0$  [48], where the *spectral abscissa* is defined as

$$\alpha_0 \doteq \sup \{ \Re(z) : z \in \mathbb{C}, h(z) = 0 \} \quad (A.3)$$

and the *characteristic polynomial* of (A.2) is

$$h(z) \doteq \det(zI - F_0 - F_1e^{-z}) = z^2 + \eta z + \eta\lambda e^{-z} \quad (A.4)$$

A sufficient and necessary condition for all roots of  $h(z)$  to lie in the open left-hand half-plane is derived in [5].

**Theorem 1** ([5], Theorem 2.1). *Let the 2-vectors  $v(b) = (pb, q - b^2)$ ,  $w(b) = (\cos b, \sin b)$ ,  $b \geq 0$ , be given. If  $r > 0$ , a necessary and sufficient condition for all roots of the equation  $h(z) = (z^2 + pz + q)e^z + r = 0$  to have negative real part is that the orthogonality condition  $v(b) \cdot w(b) = 0$ , with  $b \in \cup_{k=0}^{\infty} (2k\pi, (2k+1)\pi)$ , implies  $|v(b)| > r$ .*

From Theorem 1, (A.2) is asymptotically stable if the following implication holds for  $b \in \cup_{k=0}^{\infty} (2k\pi, (2k+1)\pi)$ :

$$\eta b \cos b - b^2 \sin b = 0 \implies \eta^2 b^2 + b^4 > \eta^2 \lambda^2 \quad (A.5)$$

In view of  $b \geq 0$  and  $\sin b \geq 0$ , (A.5) leads to (III.10) after standard algebraic manipulations, where we replace  $b$  with  $\beta = \min b \in (0, \pi/2)$ . The inequality can be rewritten as

$$\lambda < \frac{\beta}{\sin \beta} \doteq \phi(\eta) \quad (A.6)$$

where the definition of  $\phi(\cdot)$  follows from the implicit function theorem applied to  $F(\eta, \beta) \doteq \beta \tan \beta - \eta$ , which states that  $F(\eta, \beta) = 0$  if and only if  $\beta = \varphi(\eta)$  and

$$\varphi'(\eta) = \frac{\cos^2(\varphi(\eta))}{\varphi(\eta) + \sin(\varphi(\eta)) \cos(\varphi(\eta))} \quad (A.7)$$

Tedious but straightforward calculations on the first and second derivatives show that  $\phi(\eta)$  is concave increasing for any  $\eta > 0$ . The limits at 0 and  $+\infty$  can be easily computed by noting that

$$\beta_0 \doteq \varphi(0) = 0, \quad \beta_{\infty} \doteq \lim_{\eta \rightarrow +\infty} \varphi(\eta) = \frac{\pi}{2} \quad (A.8)$$

### B. Derivation of First-Order Reduced Model for Continuous-Time Double Integrators

We now show that subsystem (III.9) can be approximated to first-order dynamics when the gain  $\eta$  is sufficiently high. Let us consider (A.2) with state  $\tilde{s}(t) = [\tilde{x}(t), \tilde{z}(t)]^\top$ . Assume that the feedback gain  $\eta$  is large, so that the variable  $\tilde{z}(t)$  evolves faster than  $\tilde{x}(t)$ . We can then approximate the dynamics of  $\tilde{z}(t)$  by letting  $\tilde{x}(t-1) \equiv x_0$  be constant overtime:

$$d\tilde{z}(t) = (-\eta\tilde{z}(t) - \eta\lambda x_0)dt + dw(t) \quad (B.1)$$

Eq. (B.1) defines a standard Ornstein–Uhlenbeck process:

$$\tilde{z}(t) \sim \mathcal{N} \left( e^{-\eta t}(\tilde{z}(0) + \lambda x_0) - \lambda x_0, \frac{1}{2\eta} (1 - e^{-2\eta t}) \right) \quad (B.2)$$

In view of the time-scale separation, we assume that (B.2) holds (with  $\tilde{x}(t-1)$  constant) till  $\tilde{z}(t)$  settles at steady state:

$$\lim_{t \rightarrow +\infty} \tilde{z}(t) = \tilde{z}_{\infty} \sim \mathcal{N} \left( -\lambda x_0, \frac{1}{2\eta} \right) \quad (B.3)$$

Using (B.3), we now approximate the dynamics of  $\tilde{x}(t)$  as if  $\tilde{z}(t)$  reached the steady state instantaneously:

$$d\tilde{x}(t) \approx \tilde{z}_{\infty}dt = -\lambda\tilde{x}(t-1)dt + dn(t) \quad (B.4)$$

where the diffusion is embedded into the Brownian noise  $n(t)$  with variance proportional to  $1/\eta$ . In particular, as  $\eta \rightarrow +\infty$ ,  $\tilde{z}_{\infty} \xrightarrow{a.s.} -\lambda x_0$  and (B.4) tends to deterministic dynamics.

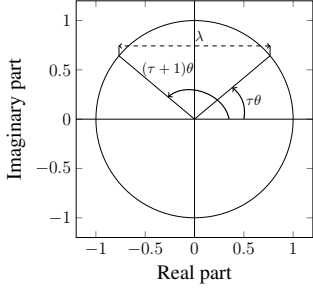


Fig. 8. A solution of (D.6) in the complex plane.

### C. Computation of Suboptimal Variance for Continuous-Time Single Integrators

The  $N$  suboptimal eigenvalues have expression (see [19])

$$\tilde{\lambda}_j^* = 2\tilde{k}^* \left( n - \sum_{\ell=1}^n \cos \left( \frac{2\pi(j-1)\ell}{N} \right) \right) \quad (\text{C.1})$$

which we write as  $\tilde{\lambda}_j^* = g_j(n)\tilde{k}^*$ . Being  $\tilde{k}^* = \tilde{\alpha}^*(n)\lambda^*$  according to Proposition 3, we write  $\tilde{\lambda}_j^* = \tilde{c}_j^*(n)\lambda^*$  with  $\tilde{c}_j^*(n) \doteq g_j(n)\tilde{\alpha}^*(n)$ . Then, each subsystem (III.3) has variance

$$\begin{aligned} \sigma_I^2(2)(\tilde{\lambda}_j^*) &= \frac{1 + \sin(\tilde{\lambda}_j^*\tau_n)}{2\tilde{\lambda}_j^* \cos(\tilde{\lambda}_j^*\tau_n)} \\ &\stackrel{(i)}{=} \frac{1 + \sin(\tilde{c}_j^*(n)\beta^*)}{2\tilde{c}_j^*(n)\beta^* \cos(\tilde{c}_j^*(n)\beta^*)} \tau_n = \tilde{C}_j^*(n)\tau_n \end{aligned} \quad (\text{C.2})$$

where (III.6) is used in (i).

### D. Stability Conditions for Discrete-Time Systems

**General Case.** In the following, we replace  $\tau_n$  with  $\tau$  for the sake of readability. For the single-integrator case, decoupling the error dynamics yields scalar subsystems of the form

$$\tilde{x}(k+1) = \tilde{x}(k) - \lambda\tilde{x}(k-\tau) + \tilde{w}(k) \quad (\text{D.1})$$

The characteristic polynomial  $h(z)$  of (D.1) is obtained by applying the lag operator  $z$  such that  $\tilde{x}(k)h(z) = \tilde{w}(k)$ :

$$h(z) = z - 1 + \lambda z^{-\tau} \quad (\text{D.2})$$

Similarly, the double-integrator decoupled subsystems are

$$\begin{aligned} \tilde{x}(k+1) &= \tilde{x}(k) + \tilde{z}(k) \\ \tilde{z}(k+1) &= (1-\eta)\tilde{z}(k) - \eta\lambda\tilde{x}(k-\tau) + \tilde{w}(k) \end{aligned} \quad (\text{D.3})$$

with characteristic polynomial

$$h(z) = z - 2 + \eta + (1-\eta)z^{-1} + \eta\lambda z^{-\tau-1} \quad (\text{D.4})$$

For positive  $\lambda$ , stability of (D.1)–(D.3) can be assessed via the Jury stability criterion, which provides necessary and sufficient conditions for the roots of (D.2) and (D.4) to lie inside the unit circle in the form of inequalities involving the coefficients of  $h(z)$ . Being these polynomial in  $\eta$  and  $\lambda$ , the Jury criterion yields  $\Theta(N\tau)$  polynomial inequalities in the feedback gains, which can be obtained through symbolic software.

**Proof of Proposition 4.** Eq. (D.2) can be studied as a root locus by varying the gain  $\lambda$ . In particular,  $\lambda = 0$  yields a

multiple root at  $z_1^* = 0$  and a simple root at  $z_2^* = 1$ . Negative values of  $\lambda$  are discarded as they push the latter outside the unit circle. As  $\lambda$  increases, the branches leave the unit ball along their asymptotes. The admissible values for  $\lambda$  are upper bounded by a threshold gain  $\lambda_{th}$  beyond which some roots leave the unit ball. In particular, we are interested in the minimum gain for which at least one root lies exactly on the unit circle. Thus, we are looking for roots of (D.2) of the form  $z = e^{j\theta}$ :

$$e^{j(\tau+1)\theta} - e^{j\tau\theta} + \lambda = 0 \quad (\text{D.5})$$

Eq. (D.5) can be equivalently written as the system

$$\begin{cases} \cos((\tau+1)\theta) - \cos(\tau\theta) + \lambda = 0 \\ \sin((\tau+1)\theta) = \sin(\tau\theta) \end{cases} \quad (\text{D.6})$$

Fig. 8 depicts a solution of system (D.6) for  $\sin(\tau\theta) > 0$ . The case  $\sin(\tau\theta) < 0$  is analogous and is omitted. Further, the solution  $(\tau+1)\theta = \tau\theta$  can be discarded from the discussion, because it implies  $\lambda = 0$  and thus prevents asymptotic stability. From elementary trigonometric arguments (c.f. Fig. 8), the second equation in (D.6) implies

$$\tau\theta + \frac{\theta}{2} = \frac{\pi}{2} + 2k\pi \longrightarrow \theta = \frac{\pi + 4k\pi}{2\tau + 1}, \quad (\text{D.7})$$

where we impose  $\theta \in [0, \pi]$  and thus  $k \in \{0, \dots, \lfloor \tau/2 \rfloor\}$ . This includes all possible cases, because the roots of (D.2) come in complex conjugates pairs. From (D.7), the first equation in (D.6), and the fact  $\cos((\tau+1)\theta) = -\cos(\tau\theta)$ , we retrieve

$$\lambda = 2 \cos \left( \frac{\pi\tau + 4k\pi\tau}{2\tau + 1} \right) \quad (\text{D.8})$$

The right-hand term in (D.8) is monotone increasing in  $k$ . Indeed, taking the argument of the cosine modulus  $2\pi$  yields

$$\frac{\pi\tau + 4k\pi\tau}{2\tau + 1} \bmod 2\pi = \frac{\pi\tau - 2k\pi}{2\tau + 1} \in \left[ 0, \frac{\pi}{2} \right] \quad (\text{D.9})$$

which is nonnegative and monotone decreasing in  $k$  for any  $\tau$ . Thus, the upper bound for the gain  $\lambda$  is given by

$$\lambda_{th} = \min_k 2 \cos \left( \frac{\pi\tau + 4k\pi\tau}{2\tau + 1} \right) = 2 \cos \left( \frac{\pi\tau}{2\tau + 1} \right) \quad (\text{D.10})$$

### E. Variance Computation for Discrete-Time Systems

**Wiener-Kintchine Formula.** Given any fixed values of delay and feedback gains, the steady-state variance  $\sigma_I^2(\lambda)$  or  $\sigma_H^2(\eta, \lambda)$  of the decoupled subsystems can be computed numerically as

$$\frac{1}{2\pi} \int_{-\pi}^{+\pi} \frac{d\theta}{|h(e^{j\theta})|^2} \quad (\text{E.1})$$

where the characteristic polynomial  $h(z)$  is (D.2) or (D.4).

**Single Integrator Model.** The moment-matching method applied to the subsystem (D.1) yields a linear system of equations in the variables  $(\rho_0, \dots, \rho_\tau)$ , where  $\rho_t \doteq \mathbb{E}[\tilde{x}(k)\tilde{x}(k \pm t)]$ :

$$\rho_0 = \mathbb{E}[\tilde{x}(k+1)^2] = \rho_0 + \lambda^2 \rho_0 + 1 - 2\lambda \rho_\tau \quad (\text{E.2a})$$

$$\rho_1 = \mathbb{E}[\tilde{x}(k+1)\tilde{x}(k)] = \rho_0 - \lambda \rho_\tau \quad (\text{E.2b})$$

⋮

$$\rho_\tau = \rho_{\tau-1} - \lambda \rho_1 \quad (\text{E.2c})$$

where (E.2b)–(E.2c) are the Yule-Walker equations. System (E.2) can be written compactly as  $A^{(\tau)}\rho = e_1$ , where  $\rho^\top = [\rho_0, \dots, \rho_\tau]$ ,  $e_1$  is the canonical vector in  $\mathbb{R}^{\tau+1}$  with nonzero first coordinate and  $A^{(\tau)} \in \mathbb{R}^{(\tau+1) \times (\tau+1)}$  with

$$A^{(\tau)} = \begin{bmatrix} -\lambda^2 & & 2\lambda \\ 1 & -1 & -\lambda \\ \ddots & \ddots & \ddots \\ -\lambda & 1 & -1 \end{bmatrix} \quad (\text{E.3})$$

In particular, when  $\tau$  is odd, the  $(\lceil \tau/2 \rceil + 1)$ -th row is

$$0 \dots 0 1 -1 -\lambda 0 \dots 0 \quad (\text{E.4})$$

while, when  $\tau$  is even, the  $(\lceil \tau/2 \rceil + 2)$ -th row is

$$0 \dots 0 1 -\lambda -1 0 \dots 0 \quad (\text{E.5})$$

Notice that  $A^{(\tau)}$  is full rank for all  $\tau \geq 1$  and thus (E.2) can be solved uniquely. In particular, we are interested in the autocorrelation  $\rho_0 = \sigma_I^2(\lambda)$ , which is given by the ratio between the minor associated with the top-left element of  $A^{(\tau)}$ , named  $n_\tau \doteq M_{1,1}^{(\tau)}$ , and the determinant  $d_\tau \doteq \det(A^{(\tau)})$ . Specifically,  $\rho_0$  is a rational function in  $\lambda$  and can be computed in closed form by a symbolic solver given any value of  $\tau$ .

Further,  $n_\tau$  and  $d_\tau$  can be computed recursively, exploiting the following nested structure of the matrix  $A^{(\tau)}$ :

$$A^{(\tau)} = \begin{bmatrix} -\lambda^2 & & -2\lambda \\ 1 & -1 & -\lambda \\ 1 & \begin{bmatrix} -1 & \\ 1 & \end{bmatrix} & \begin{bmatrix} -1 & \\ 1 & \end{bmatrix} \\ -\lambda & 1 & -1 \end{bmatrix} \quad (\text{E.6})$$

where  $\tilde{A}^{(\tau)}$  is the submatrix of  $A^{(\tau)}$  obtained by removing its first row and column such that  $M_{1,1}^{(\tau)} = \det(\tilde{A}^{(\tau)})$ , and the matrices  $\tilde{A}^{(\tau-2)}$  and  $\tilde{A}^{(\tau-4)}$  are framed in (E.6). The solution obeys the following recursive expression:

$$n_\tau = \begin{cases} (-1 - \lambda)n_{\tau-1} + \tilde{n}_{\tau-1}, & \tau \text{ odd} \\ -(1 - \lambda)n_{\tau-1} - \lambda \tilde{n}_{\tau-1}, & \tau \text{ even} \end{cases} \quad (\text{E.7a})$$

$$\tilde{n}_\tau = (2 - \lambda^2)\tilde{n}_{\tau-2} - \tilde{n}_{\tau-4} \quad (\text{E.7b})$$

$$d_\tau = d_{\tau-2} - \lambda^2(n_\tau + n_{\tau-2}) \quad (\text{E.7c})$$

$$\tilde{n}_{-3} = -1 + \lambda^2, \quad \tilde{n}_{-2} = \lambda^2, \quad \tilde{n}_{-1} = -1, \quad \tilde{n}_0 = 0 \quad (\text{E.7d})$$

$$n_{-1} = 0, \quad n_0 = 1, \quad d_{-1} = -2\lambda, \quad d_0 = 2\lambda - \lambda^2 \quad (\text{E.7e})$$

**Numerator.** We demonstrate (E.7a) for odd delays, *i.e.*,  $\tau = 2k+1, k \in \mathbb{N}$ . The other case can be obtained analogously and is thus omitted.

Let us consider the submatrix  $\tilde{A}^{(\tau)} \in \mathbb{R}^{\tau \times \tau}$  obtained by removing the first row and column of  $A^{(\tau)}$ , such that  $n_\tau = \det(\tilde{A}^{(\tau)})$ . Replacing the  $(\lfloor \tau/2 \rfloor)$ -th column with the sum of  $(\lfloor \tau/2 \rfloor)$ -th and  $(\lceil \tau/2 \rceil)$ -th columns yields

$$\det(\tilde{A}^{(\tau)}) = \begin{vmatrix} \tilde{A}_{11}^{(\tau-1)} & & \tilde{A}_{12}^{(\tau-1)} \\ \dots & 0 & -\lambda & -1 - \lambda \\ \tilde{A}_{21}^{(\tau-1)} & & 1 & 0 & \tilde{A}_{22}^{(\tau-1)} \\ & & & \vdots & \end{vmatrix} \quad (\text{E.8})$$

from which it follows  $n_\tau = (-1 - \lambda)n_{\tau-1} - \det(R^{(\tau)})$  where  $R^{(\tau)} \in \mathbb{R}^{(\tau-1) \times (\tau-1)}$  and the base case is  $n_1 = -1 - \lambda$ . This expression corresponds to (E.7a) with  $\tilde{n}_{\tau-1} = -\det(R^{(\tau)})$ . Manipulations of the second term yield a further recursive expression for  $\tilde{n}_{\tau-1}$ . Let us write

$$\det(R^{(\tau)}) = \begin{vmatrix} -1 & & -\lambda \\ 1 & \begin{bmatrix} -1 & \\ 1 & \end{bmatrix} & \begin{bmatrix} -1 & \\ 1 & \end{bmatrix} \\ \lambda & \begin{bmatrix} -1 & \\ 1 & \end{bmatrix} & \begin{bmatrix} -1 & \\ 1 & \end{bmatrix} \\ -\lambda & & 1 & -1 \end{vmatrix} \quad (\text{E.9})$$

where the two inner boxes highlight  $R^{(\tau-2)}$  and  $R^{(\tau-4)}$ , respectively. Straightforward calculations yield

$$\det(R^{(\tau)}) = \det(R^{(\tau-2)}) + \begin{vmatrix} 1 & \begin{bmatrix} -1 & \\ 1 & \end{bmatrix} & \begin{bmatrix} -1 & \\ 1 & \end{bmatrix} \\ \lambda & \begin{bmatrix} -1 & \\ 1 & \end{bmatrix} & \begin{bmatrix} -1 & \\ 1 & \end{bmatrix} \\ -\lambda & & 1 & -1 \end{vmatrix} \quad (\text{E.10})$$

The determinant in the second addend is computed as

$$-\lambda \det(R^{(\tau-2)}) + \begin{vmatrix} 1 & \begin{bmatrix} -1 & \\ 1 & \end{bmatrix} & \begin{bmatrix} -1 & \\ 1 & \end{bmatrix} \\ -\lambda & & 1 \end{vmatrix} \quad (\text{E.11})$$

and the second addend in the above equation has the same structure as the determinant in the second addend in (E.10). Thus, an easy inductive argument proves

$$\begin{aligned} \det(R^{(\tau)}) &= \det(R^{(\tau-2)}) + \lambda \left( -\lambda \det(R^{(\tau-2)}) \right. \\ &\quad \left. - \lambda \det(R^{(\tau-4)}) - \dots - \lambda \det(R^{(3)}) - \lambda \right) \end{aligned} \quad (\text{E.12})$$

where the base case is  $\det(R^{(3)}) = -\lambda^2$ . Eq. (E.7b) is

retrieved by noting

$$\det(R^{(\tau-2)}) - (1 - \lambda^2) \det(R^{(\tau-4)}) = \lambda \left( -\lambda \det(R^{(\tau-6)}) - \dots - \lambda \right) \quad (\text{E.13})$$

and thus the tail of the summation in (E.12) can be replaced by the left-hand term in (E.13).

**Denominator.** The denominator of  $\rho_0$  is computed as the determinant of  $A^{(\tau)}$ . From (E.3) we get

$$\det(A^{(\tau)}) = -\lambda^2 M_{1,1}^{(\tau)} - 2\lambda \left| \begin{array}{ccccc} 1 & -1 & & & \\ & 1 & -1 & & -\lambda \\ & & 1 & \boxed{\tilde{A}^{(\tau-4)}} & \\ & & & & 1 \\ 2\lambda & & -\lambda & & 1 \end{array} \right| \quad (\text{E.14})$$

where  $\tilde{A}^{(\tau-2)}$  and  $\tilde{A}^{(\tau-4)}$  are framed in the second addend above. The latter can be computed as the following sum:

$$\lambda M_{1,1}^{(\tau-2)} + \left| \begin{array}{ccccc} 1 & -1 & & & \\ & 1 & \boxed{\tilde{A}^{(\tau-4)}} & & \\ & & & & 1 \\ & & -\lambda & & \\ & & & & 1 \end{array} \right| \quad (\text{E.15})$$

where the same structure is repeated recursively in the second addend above. Thus, an easy inductive argument proves

$$d_\tau = -\lambda^2 n_\tau - 2\lambda(\lambda n_{\tau-2} + \lambda n_{\tau-4} + \dots + \lambda n_1 + 1) \quad (\text{E.16})$$

where the base case is  $d_1 = -\lambda^2(-1 - \lambda) - 2\lambda$ . Eq. (E.7c) is retrieved by noting

$$\begin{aligned} -2\lambda(\lambda n_{\tau-2} + \lambda n_{\tau-4} + \dots + 1) &= \\ -\lambda^2 n_{\tau-2} - \lambda^2 n_{\tau-2} - 2\lambda(\lambda n_{\tau-4} + \dots + 1) &= \\ -\lambda^2 n_{\tau-2} + d_{\tau-2} \end{aligned} \quad (\text{E.17})$$

Given  $\tau$ , convexity of  $\rho_0$  in  $\lambda$  can be assessed by checking the sign of the second derivative in the stability region. This reduces to a system of inequalities which can be solved, *e.g.*, by `solve_rational_inequalities` in Python. The variance was proved strictly convex for all tried delays.

is composed of the following equations:

$$\begin{aligned} \rho_0 &= (2 - \eta)^2 \rho_0 + (1 - \eta)^2 \rho_0 + \eta^2 \lambda^2 \rho_0 + 1 \\ &\quad - 2(2 - \eta)(1 - \eta) \rho_1 - 2(2 - \eta) \eta \lambda \rho_{\tau+1} \\ &\quad + 2(1 - \eta) \eta \lambda \rho_\tau \end{aligned} \quad (\text{E.18a})$$

$$\rho_1 = (2 - \eta) \rho_0 - (1 - \eta) \rho_1 - \eta \lambda \rho_{\tau+1} \quad (\text{E.18b})$$

$$\rho_2 = (2 - \eta) \rho_1 - (1 - \eta) \rho_0 - \eta \lambda \rho_\tau \quad (\text{E.18c})$$

⋮

$$\rho_{\tau+1} = (2 - \eta) \rho_\tau - (1 - \eta) \rho_{\tau-1} - \eta \lambda \rho_1 \quad (\text{E.18d})$$

where (E.18b)–(E.18d) are the Yule-Walker equations associated with (D.3). Analogous considerations to the single-integrator model can be done in this case.

**Double Integrator Model.** The moment-matching system associated with (D.3) has  $\tau + 2$  variables  $(\rho_0, \dots, \rho_{\tau+1})$  and